

N85-22511

MASS SPECTRA OF NEUTRAL PARTICLES RELEASED DURING ELECTRICAL
BREAKDOWN OF THIN POLYMER FILMS*

B. R. F. Kendall
The Pennsylvania State University
University Park, Pennsylvania 16802

Little is known of the composition of the neutral particle flux released during the electrical breakdown of polymer films. Mass spectrometric analysis of the particles is unusually difficult because of the transient nature of the event, the unpredictability of its exact position and timing, and the very large amount of information generated in a period as short as one microsecond. A special type of time-of-flight mass spectrometer triggered from the breakdown event has been developed to study this problem. Charge is fed onto a metal-backed polymer surface by a movable smooth platinum contact. A slowly increasing potential from a high-impedance source is applied to the contact until breakdown occurs. The breakdown characteristics can be made similar to those produced by an electron beam charging system operating at similar potentials. With this apparatus it has been shown that intense instantaneous fluxes of neutral particles are released from the sites of breakdown events. For Teflon FEP films of 50 and 75 microns thickness the material released consists almost entirely of fluorocarbon fragments, some of them having masses greater than 350 amu (atomic mass units), while the material released from a 50 micron Kapton film consists mainly of light hydrocarbons with masses at or below 44 amu, with additional carbon monoxide and carbon dioxide. The apparatus is being modified to allow electron beam charging of the samples.

INTRODUCTION

Because of the scarcity of data on the composition of the neutral and ion fluxes from dielectric breakdown events on spacecraft, mass spectrometric analyses of these fluxes are particularly important.

Mass analysis of particles from an electrical breakdown involves a particularly difficult set of constraints. The event occurs essentially at a point in space and at an instant in time. The exact position and timing of the event are not known in advance. The event produces a swarm of neutral molecules, molecular clusters and ions of different masses which radiate from the breakdown site over a wide range of speeds and directions. At a distance greater than a few cm from the breakdown site the particle number density is likely to be quite low and falling rapidly because of both speed variations and angular dispersion. The expanding gas and ion burst will pass any given point in a time much shorter than the time taken for any conventional mass spectrometer to scan once through its mass range.

*Supported by NASA Grant NSG-3301.

The difficult experimental conditions listed above make it essential to use a mass spectrometer in which a maximum amount of output data can be obtained in the shortest possible time. This effectively limits the choice of spectrometer types to those in which all of the ions leaving the ion source become part of a recorded output signal. It was decided that a specially designed time-of-flight mass spectrometer offered the most cost-effective solution.

MASS SPECTROMETER

The time-of-flight mass spectrometer and the vacuum chamber used for its development are shown in Figure 1. The pulsed two-field ion source (ref. 1) is on the left. Incoming molecules are ionized by an electron beam inside the ion source and the resulting ions are accelerated in approximately monoenergetic bunches into the flight tube. The ions therefore reach the ion detector in ascending order of mass, according to the formula

$$t = s(m/2eV)^{1/2}$$

where t is the flight time through the flight tube, s is the length of the flight tube, m is the ion mass, e is the ion charge, and V is the potential difference through which the ions fall inside the source. With a 115cm flight tube and 300V accelerating potential, the flight time of an ion of mass 100 amu is approximately 47μsec.

A segmented cylindrical lens focuses the ion beam and centers it on the input of the ion detector. The flight tube is operated at ground potential, rather than at high potentials as in most time-of-flight mass spectrometers, in order to minimize electrostatic interactions with the sample charging apparatus. An electron multiplier ion detector is used for high sensitivity and fast response.

It follows from the equation for the flight time of an ion that the electrical signals leaving the ion detector represent a series of complete mass spectra, each one having the corresponding source pulse at its $t=0$ point. Any number of successive spectra can be displayed, from a single spectrum up to as many as 100 spectra per millisecond. A typical mass spectrum of residual gases in the vacuum chamber is shown in Figure 2. Special techniques are needed for operation at repetition intervals faster than the ion flight times (ref. 2) and for displaying the rapidly-changing spectra (refs. 3, 4).

This mass spectrometer was originally intended for remote operation inside a N.A.S.A. space simulation chamber which already contained the necessary electron beam charging and sample monitoring equipment. These plans had to be changed when it was discovered that the operational lifetime of the sensitive electron multiplier ion detector was unacceptably short in this chamber, apparently because of oil contamination traceable to the early history of its diffusion-pumped vacuum system.

A partial redesign was made to allow electrical breakdown experiments to be done in the turbo-molecular-pumped chamber which had been used for the original development of the mass spectrometer (fig. 3). This solved the oil contamination problem but imposed other difficulties because of the small volume and pumping

capacity. The first experiments have been done with a simple contact device feeding charge onto the insulating surface. At the same time a miniaturized electron beam charging system is being developed.

DIRECT-CONTACT EXPERIMENTS

Figure 4 shows the charging apparatus. Electrons are fed onto the insulating surfaces from a smooth platinum contact. A slowly increasing negative potential from a high-impedance, low-capacitance source is applied to the contact until breakdown occurs. The sample is held in place on a perforated, rotatable 9cm disc by a circumferential retaining ring.

The discharge current waveforms, peak currents, and surface damage characteristics obtained with this apparatus can be made similar to those produced by a high-voltage electron beam charging system by choosing a suitable length (about 45 cm) of coaxial cable as an energy storage line. A useful feature is that, by progressively rotating the sample beneath the contact, the observed gas bursts can be correlated with actual discharge sites left behind on the sample, which can then be removed and observed under an optical or electron microscope. Discharges normally occur within about 4mm of the contact. Few occur directly beneath the contact. Breakdown voltages are similar to those obtained with a monoenergetic electron beam charging system.

The samples tested in the direct-contact experiments were Teflon FEP and Kapton H films of 50 and 75 micron thicknesses. They were metallized on one side with silver overlaid by an Inconel protective coating. No adhesive backing was used.

The first tests with Teflon samples showed that an intense burst of neutral fragments was being released from each discharge. A large number of peaks representing Teflon fragments of the form $C_xF_y^+$ could be seen in each mass spectrum.

The variation with time of the number density of these Teflon fragments was obtained by using the mass peak amplitude signals to intensify a cathode-ray oscilloscope trace, producing an array of dots. By deflecting this display downwards, a semiquantitative indication of the various changes in number densities was obtained. Such a display is shown in Figure 5 with the major peaks identified. A background spectrum is included for comparison.

Close examination of these and other similar records showed that release of neutral particles often began just before breakdown with production of hydrocarbons, followed by a burst of fluorocarbons during the actual breakdown. Hydrocarbons are visible in the lower left photograph in Figure 5. Both hydrocarbon and fluorocarbon concentrations then fall with a time constant of about 120 msec, determined by the volume and pumping speed of the vacuum system. The hydrocarbon peaks are probably caused by adsorbed surface impurities. Further work is required to establish their origins.

The most intense fluorocarbon peak corresponds to CF_3^+ but ions up to and beyond $C_5F_9^+$ are present. Switching off the ionizing electron beam in the mass spectrometer ion source causes these peaks to disappear, showing that they are ionization products of even larger neutral fragments and not ions released directly

from the discharge. Far more of these heavy ions were observed than are present in the mass spectrum of the heaviest fluorocarbons for which published data are available (C_6F_{14}), suggesting that very large neutral fragments, of mass much greater than 350 amu, were leaving the Teflon surface during the discharge.

After completion of the Teflon tests, a 50 micron Kapton film with metal backing was installed in the apparatus and a new series of breakdown measurements was begun. Results were very different. The Kapton produced only light fragments, giving rise to mass spectra containing mainly masses 44, 28, and 15, as shown in the intensity-modulated spectrum of Figure 6. It appears that the mass 44 peak represents CO_2^+ and $C_3H_8^+$; mass 28 is CO^+ and $C_2H_4^+$, and mass 15 is CH_3^+ . It should be noted that Kapton contains a substantial amount of oxygen.

In general breakdown voltages were higher for a given thickness of Kapton than with Teflon.

Figure 7 shows the chemical structure of Teflon and Kapton. The origins of many of the observed fragment ions (formed in the mass spectrometer ion source by electron bombardment of even larger polymer fragments released by the discharge) are obvious.

HIGH SPEED RECORDING

High-resolution mass spectra are generated at such a rate in this experiment (up to 10^5 /sec.) that even modern digital recorders are barely adequate for following complex events. Photographic techniques have been used almost exclusively to date. Examples are the intensity-modulated displays of Figures 5 and 6. When quantitative measurements of peak heights are desired an offset raster display is used as in Figures 8 and 9. Here successive conventional mass spectra (in this case 16 per group) are superimposed upon one another, after which the oscilloscope trace moves upwards and to the right for display of the next group. Figure 8 shows the background gases in the absence of breakdown, and Figure 9 shows the burst of light gases and polymer fragments from the breakdown of a 50 micron Kapton film.

ADDITIONAL RESULTS

Items (1) - (3) of Figure 10 summarize the results of the experiments described above. The figure also shows five additional phenomena which have been identified and studied.

Secondary discharges were seen on several occasions. Electrical breakdowns were triggered at distances up to 15cm from the site of a Teflon film breakdown. In some cases the metallic electrodes between which the secondary discharge occurred were operating at less than 65% of their normal breakdown potential difference. Triggering is presumably caused by the burst of neutral and ionized material from the polymer breakdown site. The effect probably occurs also with Kapton, but this has not been checked. This phenomenon has been seen with both electron beam and direct charging of the sample.

Direct transfer of Teflon fragments is obviously likely because of the large fragments observed in the mass spectrum. It has been confirmed by the formation of insulating layers near the breakdown site and by instantaneous changes in the secondary electron emission coefficient of surfaces up to 100cm away. Partial recovery occurs over a period of several days. The effect does not appear to occur with Kapton, but this point needs further study.

Indirect transfer of Teflon has similar effects. It appears to be the result of Teflon fragments striking an intervening surface and then being almost instantaneously re-emitted into areas which are not on a direct line of sight from the discharge.

Removal of metal from the backing film was detected with Kapton samples. In some cases the Kapton film remained intact above the damage site. The effect is originally observable only under magnification but after several months in air the holes are easily visible with the naked eye because of local discoloration of the Kapton.

Photon-induced desorption and electron-induced desorption of adsorbed gases from surfaces near discharge sites are to be expected and have been observed. The effect is not directly linked with the presence of a polymer film, since any spark could supply the necessary photons and electrons. The effect is about one order of magnitude smaller than the direct gas evolution from polymer film breakdowns.

CONCLUSIONS

Many of the phenomena listed in Figure 10 could have significant effects on spacecraft surfaces. Jets of heavy polymer fragments from Teflon discharge sites could form insulating layers on adjacent electrodes, could act as triggers for gas discharges, and could change the secondary electron emission properties of distant surfaces. The much lighter fragments from Kapton may also be capable of triggering remote discharges. The ejection of material from the conducting backing of polymer films may result in metallic contamination of nearby insulation. Photon-induced and electron-induced desorption of gas from surfaces adjacent to a discharge site also occurs and adds to the intensity of the observed neutral-particle pulses.

REFERENCES

1. Wiley, W. C. and McLaren, I. H. : Time-of-Flight Mass Spectrometer with Improved Resolution, Rev. Sci. Instrum. 26, pp 1150-1157 (1955).
2. Kendall, B. R. F. : Automatic Data Processing for a Sensitive Time-of-Flight Mass Spectrometer, Jour. Sci Instrum. 39, pp 267-272 (1962).
3. Meyer, R. T. : Fast Recording Techniques for Time-Resolved Mass Spectrometry; in "Time-of-Flight Mass Spectrometry" (ed. D. Price and J. E. Williams), Pergamon Press, London, 1969, pp 61-87.
4. Lincoln, K. A. : Data Acquisition Techniques for Exploiting the Uniqueness of the Time-of-Flight Mass Spectrometer: Application to Sampling Pulsed Gas Systems; in "Dynamic Mass Spectrometry" (ed. D. Price and J. F. J. Todd), Heyden and Son, London, 1981, pp 111-119.

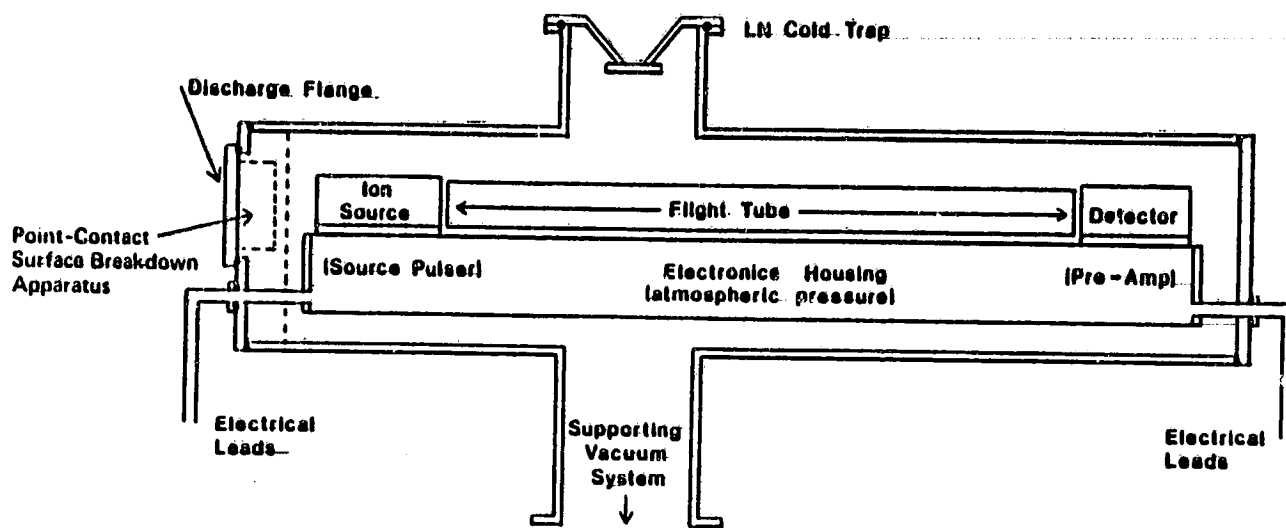


Figure 1. - Physical layout of TOFM's.

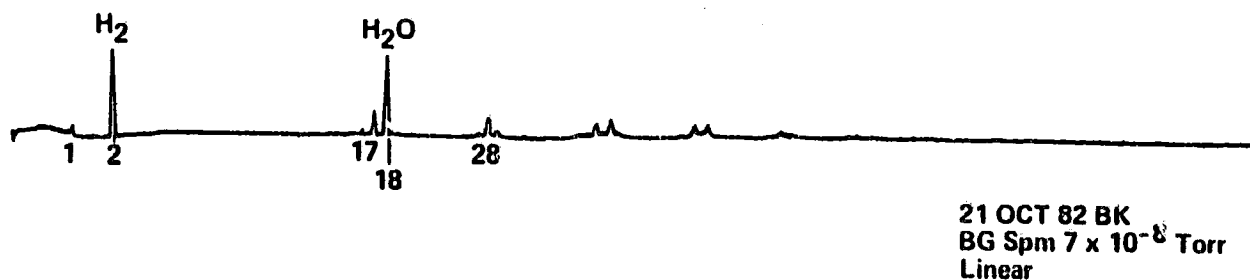


Figure 2. - Mass spectrum of background gases in vacuum chamber.

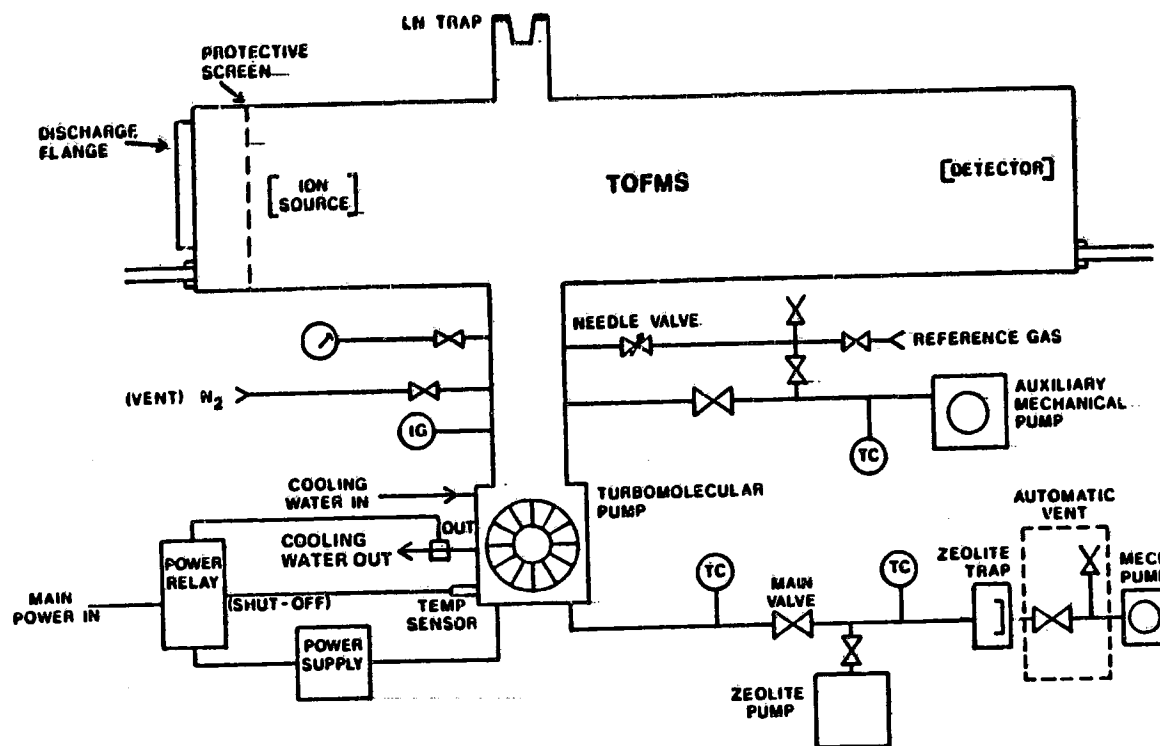


Figure 3. - General layout of vacuum system.

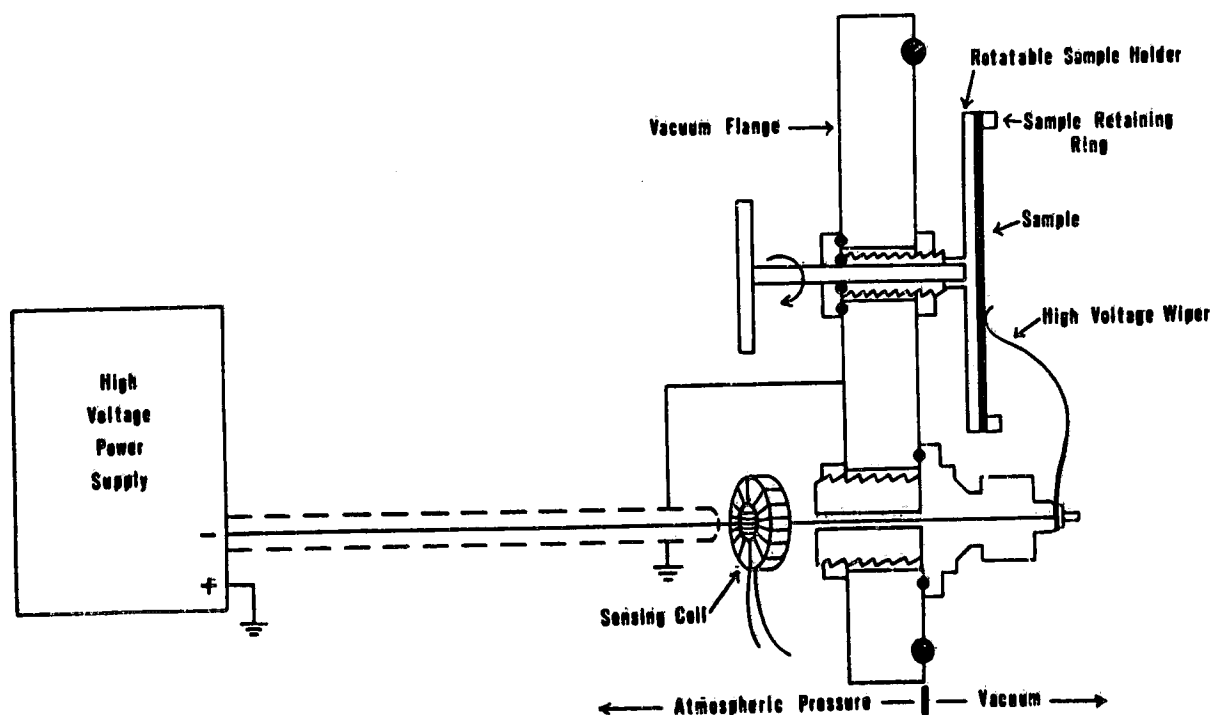


Figure 4. - Point-contact surface breakdown apparatus.

ORIGINAL PAGE IS
OF POOR QUALITY

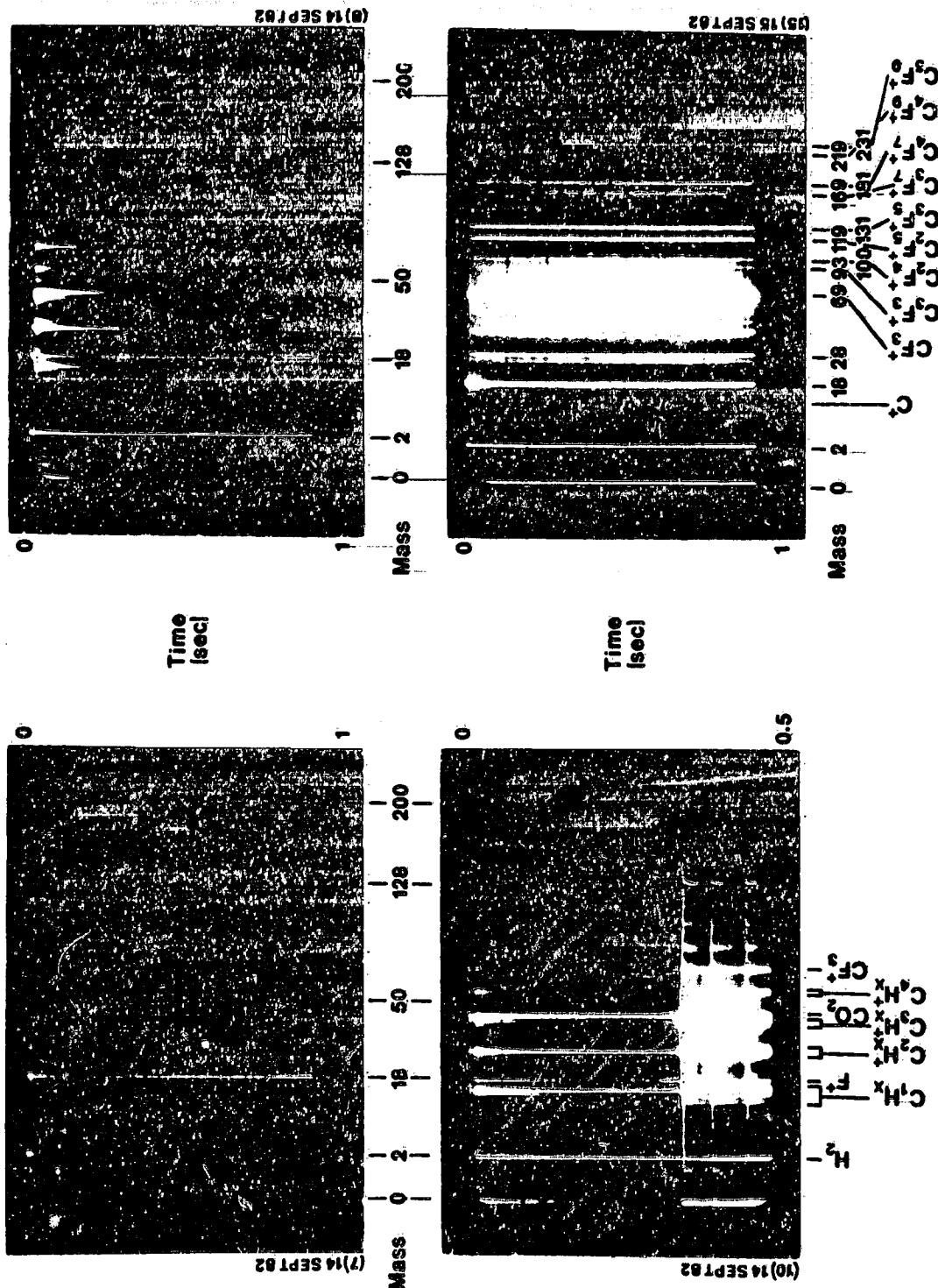


Figure 5. - Variations with time of intensity-modulated mass spectrum associated with point-contact breakdown of 50 μ Teflon layer.

Upper Left: Background spectrum, no breakdown, 9x10⁻⁸ Torr.
 Upper Right: Breakdown at 13 kV. Approx. 0.01 J.
 Lower Left: Breakdown at 16 kV. Multiple strike.
 Lower Right: Continuous discharge through spark-damaged area of surface at 12-13 kV.

ORIGINAL PAGE IS
OF POOR QUALITY

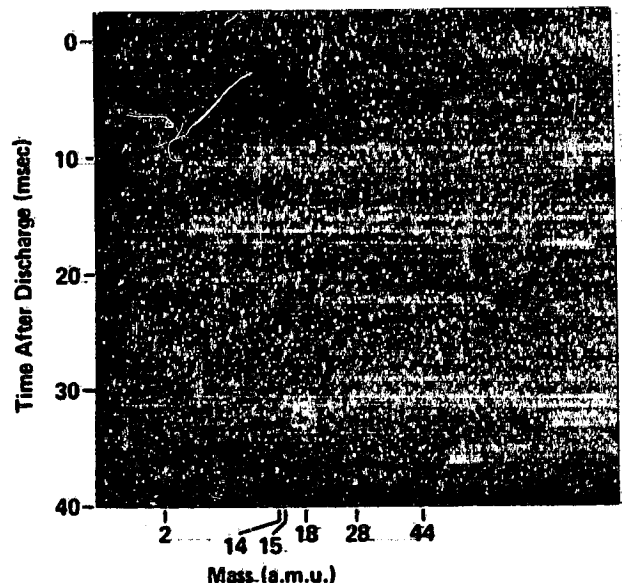


Figure 6. - Intensity-modulated raster display for breakdown of 50 micron Kapton film at 18 kV. Main peaks 44 (CO_2^+ , C_3H_8^+), 28 (CO^+ , C_2H_4^+), 15 (CH_3^+).

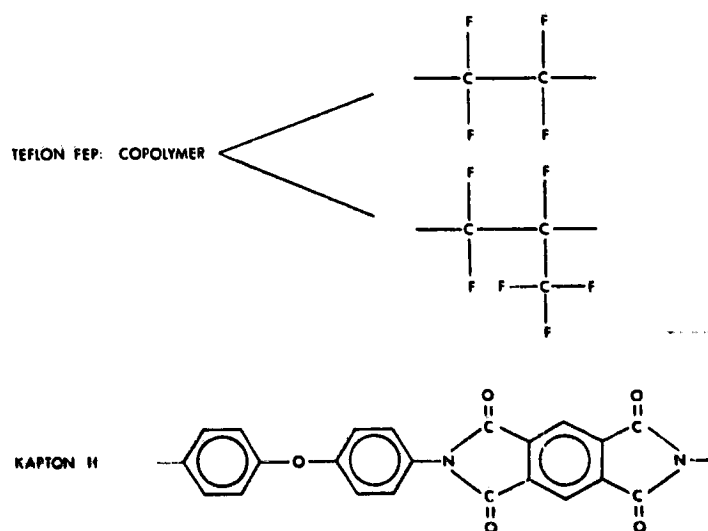


Figure 7. - Polymer structures. Hydrogen bonds omitted in Kapton structure for clarity.

ORIGINAL PAGE IS
OF POOR QUALITY

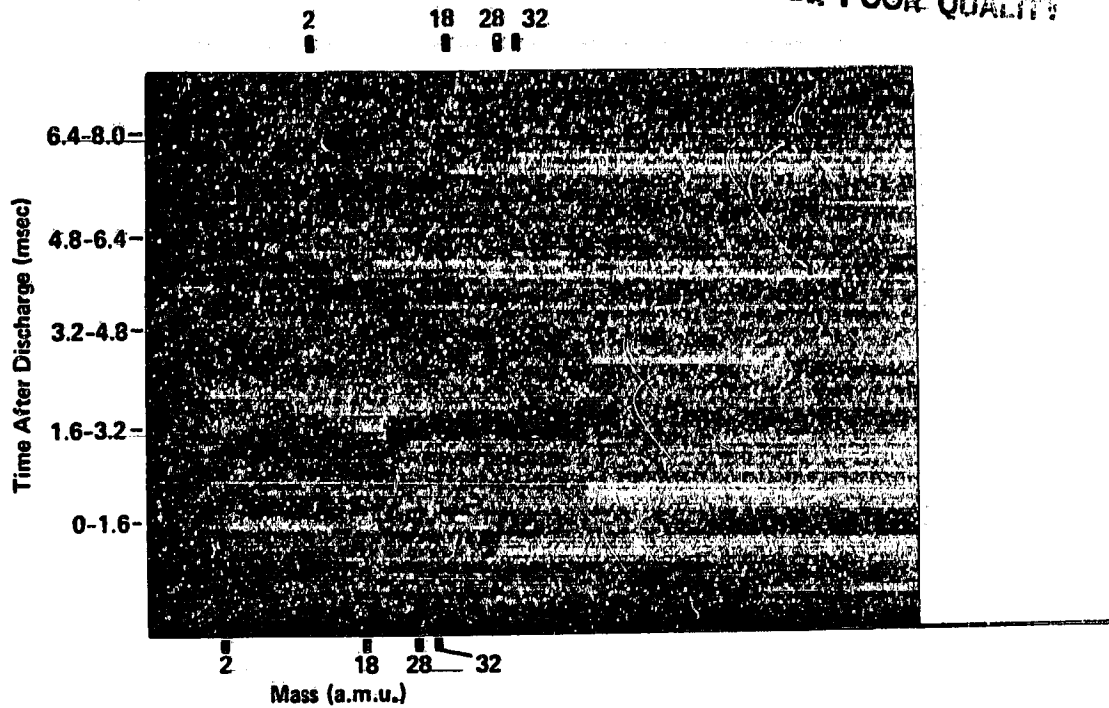


Figure 8. - Background gas spectrum (no discharge). Offset multitrace raster display, 16 spectra per trace.

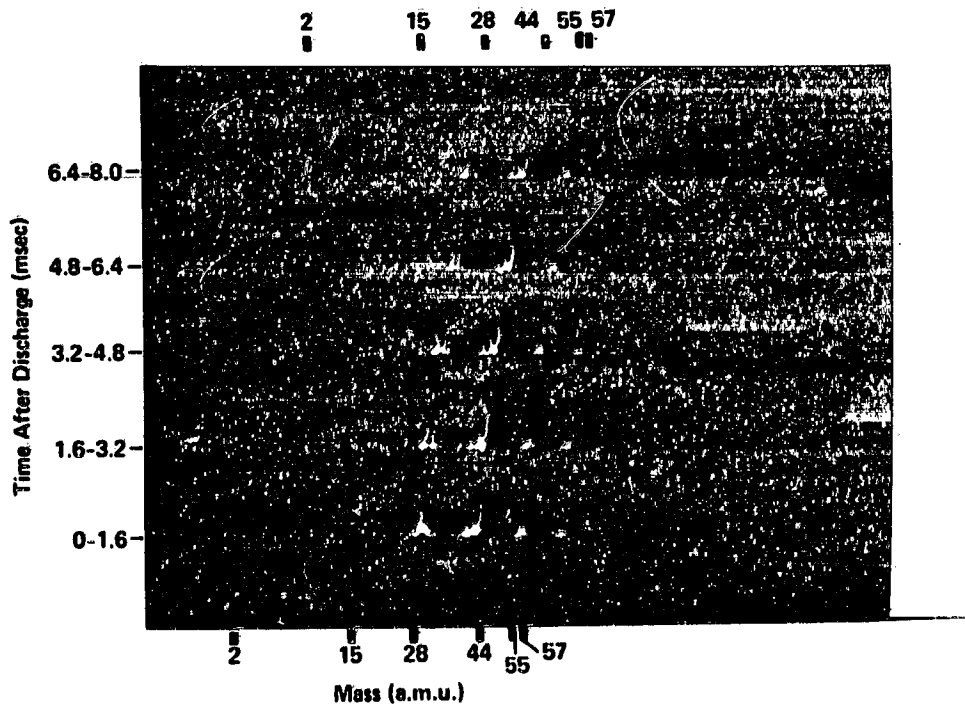


Figure 9. - Contact discharge through 50 μ Kapton film at 16 kV. Offset multi-trace raster display, 16 spectra per trace.

PHENOMENON	POLYMER	SYMBOLIC REPRESENTATION	COMMENTS
1. Intense neutral-particle pulse	Teflon Kapton		Easily detectable by fast ion gauge.
2. Emission of heavy fragments	Teflon		> 350 amu
3. Emission of light fragments	Kapton		< 44 amu
4. Secondary discharge	Teflon		Gases emitted from electrode surfaces.
5. Direct material transfer	Teflon		Change in secondary emission characteristics.
6. Indirect material transfer	Teflon		As for (5).
7. Removal of metal backing	Kapton		
8. Photon-induced desorption Electron-induced desorption	—		CO ₂ , CO, H ₂ , H ₂ O, CH ₄

Figure 10. -Neutral-particle phenomena observed during electrical breakdown of polymer films (contact charging). Insulating side of metal-backed polymer films indicated by (P).